

## **Preliminary Analysis of In-reactor Behavior of Three MOX Fuel Rods in the Halden Reactor**

Yang-Hyun KOO, Byung-Ho LEE and Dong-Seong SOHN

Korea Atomic Energy Research Institute  
P.O. Box 105, Yusong, Taejeon, Korea, 305-600

### **Abstract**

Preliminary analysis of in-reactor thermal performance of three MOX fuel rods, which are going to be irradiated in the Halden reactor beginning in the first quarter of the year 2000 under the framework of the OECD Halden Reactor Programme, have been conducted by using the computer code COSMOS to ensure their safe operation. Parametric studies have been carried out to investigate the effect of uncertainties on in-reactor behavior by considering the four kinds of uncertainties; thermal conductivity, linear power, manufacturing parameters, and model constants. The analysis shows that, in the case of annular MOX-1 fuel, calculation results for thermal performance vary widely depending on the selection of model constants for fission gas release (FGR). On the contrary, the thermal performance of solid MOX-3 fuel does not depend on the choice of FGR constants to a large extent as MOX-1, because the fuel temperature is very high in the MOX-3 irrespective of the choice of FGR constants and hence the capacity of grain boundaries to retain gas atoms is not large enough to accommodate the number of gas atoms reaching the grain boundaries. It is planned that when the data on microstructure and thermal conductivity for each type of MOX fuel are available, new analysis will be made using these information. In addition, FGR model constants will be derived from the measured fuel centerline temperature, rod internal pressure and other related data.

### **1. Introduction**

An irradiation test with three MOX fuel rods and three Inert Matrix Fuels (IMF) rods is going to be carried out in the Halden reactor from the beginning of the year 2000 under the framework of the OECD Halden Reactor Programme (HRP). The purpose of this irradiation test is to investigate the overall in-reactor thermal performance of MOX and IMF fuel fabricated with different processes and also to generate in-pile data under irradiation conditions similar to those of current LWRs. To ensure the safe irradiation of three MOX and three IMF rods in the Halden reactor, it is required to carry out a preliminary analysis of their in-reactor behaviors. The present analysis will be made for three MOX fuel rods in which KAERI is interested by using the compute code COSMOS [1].

### **2. Instrumentation and geometry**

The three MOX fuel rods will be instrumented with expansion thermometers (ET), while each of the other three ones will have a thermocouple (TC) at the top end of the fuel stack and a pressure transducer (PF) at the bottom end to measure fuel centerline temperature and fuel internal pressure (fission gas release) during irradiation. All the fuel pellets of MOX-1 and MOX-2 fuel rods will have a central hole of 1.8 mm in diameter for the installation of the expansion thermometer. On the other hand, in MOX-3 only 4 pellets at the top end of the fuel stack will be drilled for the installation of a thermocouple (Table 1).

Fig.1 shows the radial view of the six test rods, cable tube and neutron detectors (ND) in the rig that will contain three MOX and three IMF test rods. The five vanadium (Va) neutron detectors instrumented in the rig are used to calculate the power generated in the test rig and ultimately the power produced in each rod.

Table 1. Different fabrication methods and instrumentations for six MOX test rods [2].

	MOX-1	MOX-2	MOX-3	IMF-1	IMF-2	IMF-3
Fuel Form	MOX	MOX	MOX	IMF	IMF	IMF
Fabrication Method	SBR	Dry mill	Dry mill	Dry mill	Dry mill	Co-precipitation
Instrumentation	ET	ET	TC, PF	TC, PF	ET	TC, PF
Rig Position	1	3	4	2	5	6

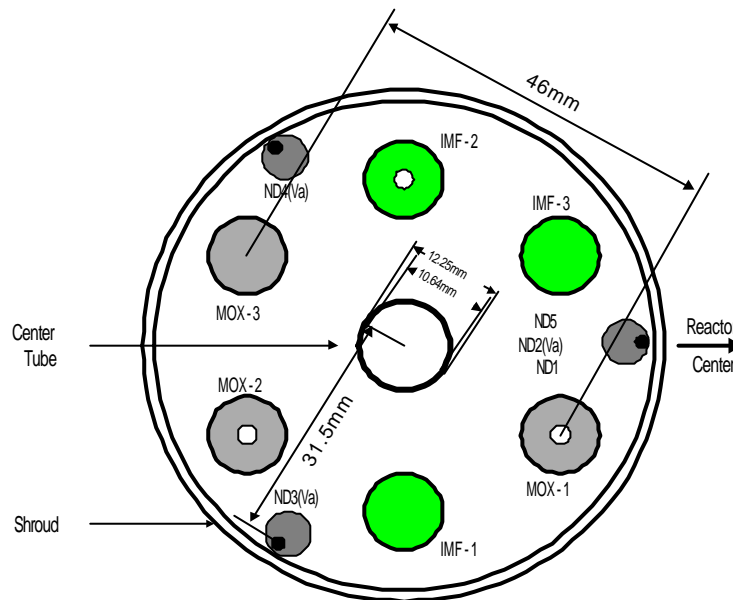


Fig.1. Radial view of the test rig to be used for the MOX/IMF irradiation [3].

### 3. Input

#### 3.1. Manufacturing parameters

Since the fabrication and characterization of MOX-2 and MOX-3 fuel rods are not yet finished, final manufacturing parameters for these two rods are not available at the moment. Therefore, manufacturing parameters for these two rods given in Table 2 are obtained from the draft drawing and the pellet dimension prepared by KAERI for the Halden test [4]. Manufacturing parameters for the MOX-1 supplied by a foreign fuel company are taken from a Halden internal memo [5].

Table 2. Manufacturing parameters of three MOX fuel rods.

	MOX-1	MOX-2	MOX-3
Pellet			
• Outer diameter (mm)	8.194±0.012	8.19±0.013	8.19±0.013
• Inner diameter (mm)	1.8	1.8	0.0
• Height (mm)	12.145±0.217	10.0±1.5	10.0±1.5
• Density (% TD)	94.6±0.37	95.0±1.36	95.0±1.36
• Stack length (mm)	500	500	500
Cladding			
• Outer diameter (mm)	9.50	9.50	9.50
• Inner diameter (mm)	8.36	8.36	8.36
Rod			
• Radial gap size ( $\mu$ m)	83.0	85.0	85.0
• He fill pressure (bar)	4.0	4.0	4.0

### 3.2. Power history

The preliminary power history for three MOX rods generated by KAERI's neutron physics group [6] is given in Fig.2. Average linear powers for the three MOX rods are given as a function of effective full power days (EFPD). Since 100 EFPD approximately corresponds to one cycle and it is usually possible to achieve two cycles per year in the Halden reactor, it would take about five years to complete the full planned irradiation shown in Fig.2.

Since this is the first irradiation of the MOX and IMF fuel of this current type, linear power during the first cycle should be sufficiently low to prevent any unexpected failure of the test rods. Therefore, the linear power in the first cycle is chosen not to exceed 250 W/cm. The maximum linear power of 340 W/cm in the second cycle was determined in such a way that it does not exceed the local limiting linear power permissible in currently typical PWRs under steady-state and operational transient conditions, which is for example 666 kW/cm for 14x14 fuel assembly [7] when a radial power peaking factor of 1.55 and an axial power peaking factor of around 1.25 are considered. These two power peaking factors are normally used for the design of UO<sub>2</sub> fuel loaded into Westinghouse-type PWRs.

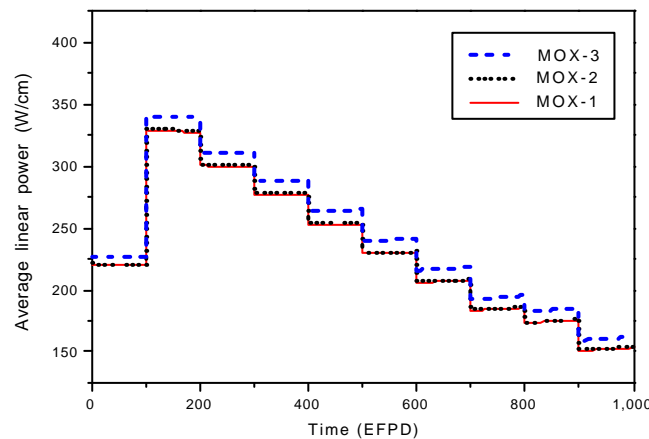


Fig.2. Average linear powers of MOX-1, MOX-2, and MOX-3 versus time (EFPD)

### 3.3. Radial power depression

Fig.3 shows the radial power density distributions in the MOX-1 rod as a function of pellet average burnup [8]. Generally, radial power depression in MOX pellet is different from that in conventional LWR  $UO_2$  pellet because of the following two factors. First, neutron spectrum obtained from Pu fission is harder than that for  $UO_2$  fuel leading to longer migration distance of thermal neutrons in the MOX pellet until they are mostly absorbed by Pu isotopes or U-238. Second, due to a rather higher total Pu content of about 6 to 8 wt%, the amount of U-238 contained in the MOX fuel is obviously less than that in typical  $UO_2$  and hence this creates a lesser amount of Pu-239 from U-238. Furthermore, two more things in the Halden reactor influence the radial power depression. First, heavy water that is being used as a moderator in the Halden reactor compared with light water in LWR, yields a different neutron spectrum due to less effective moderation ability of heavy water. In addition, fuel-to-moderator ratio, which also determines the degree of moderation of fission neutrons, is different from that used in typical commercial LWR. The combination of these four factors produces the radial power depression in the Halden reactor that is shown in Fig.3 for MOX pellet containing total Pu content of about 8 wt%.

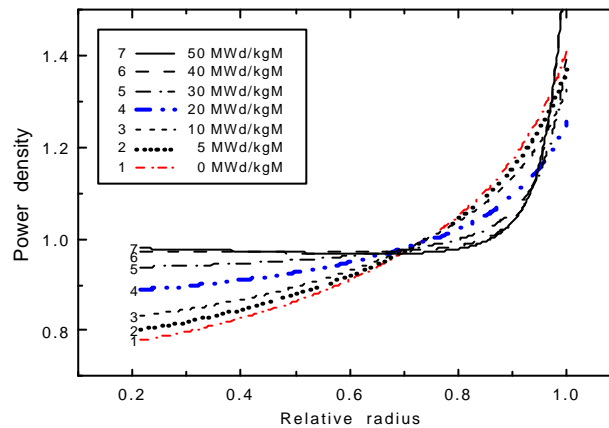


Fig.3. Radial power density distributions in the MOX-1 as a function of pellet average burnup.

### 3.4. Axial power profile

Typical axial profile of thermal neutron flux in the Halden reactor can be described by a chopped cosine shape over fuel stack length. One of these examples can be seen in Fig.3 and Fig.4 of HWR-605 [9]. Using the assumption that maximum linear power in the center of fuel stack is 1.05 times as large as the average linear power [9], the respective average power for each segment is derived when the fuel stack is divided into three parts with equal length. The calculated average power in three segments is  $0.9774 \bar{p}$  for upper and lower segments and  $1.0443 \bar{p}$  for middle segment, respectively, where  $\bar{p}$  is the rod average linear power.

### 3.5. Fast neutron flux

Fast neutron flux is needed to calculate irradiation-induced cladding creep. The fast neutron flux in the Halden reactor is described as follows [10]:

$$\text{Fast neutron flux (nol cm}^2 \cdot \text{s)} = 10^{10} \cdot \text{linear power (W/cm)} \cdot \text{No of fuel rods in a rig}$$

### 3.6. Model constants

Since this is the first time that the current type of MOX fuel is irradiated in a nuclear reactor, model constants of this fuel for pellet relocation, densification, swelling, fission gas release and so on are not available at present. The model constants for cladding creep that depends on the manufacturing method and microstructure of the cladding to be used in the present test, are also unclear. Therefore, it is assumed that the model constants for pellet relocation and cladding creep are the same as those used for  $UO_2$  fuel. As for the model constant for densification, which is defined as the maximum volume reduction, 1.8% is used for the present MOX. This value is the average value of  $\sim 1.2\%$  for Rod 10 and  $\sim 2.3\%$  for Rod 11 in the Halden experiment IFA 597.4/5 [9]. The swelling rate of  $0.5\% \Delta V/V$  per 10 MWd/kgMOX [9] is used for the present analysis.

Three FGR models [11,12,13] available have been compared to investigate which one is most suitable for the analysis of the three MOX test rods by using case 14 in Table 3 for the MOX-1. Reasonable values of thermal conductivity for MOX fuel, linear power and manufacturing parameters are selected for this calculation. However, model constants are chosen in such a way that the combination of these constants leads to the highest fuel centerline temperature so that calculated centerline temperatures of the MOX-1 exceed the 1% threshold temperature.

The centerline temperature in Fig.4 is one for the middle segment of the MOX-1. It is shown here that, for the model constants of 0.25 and 0.05 for  $f_b^{FBX}$  and  $(\Delta V/V)_e^{FBX}$ , once the fuel centerline temperature exceeds the threshold temperature for FGR at about 370 EFPD, gas release increases rapidly via the diffusion-dominant mechanism. This suggests that the FGR model of Koo et al. [11] is a reasonable one in that it can predict diffusional gas release for fuel temperatures higher than threshold temperature [16]. This gas release in turn aggravates the gap conductance leading to higher fuel temperature and more release. On the contrary, when the centerline temperature decreases, release fraction also decreases due to the fact that even if gas release exists, the released amount is relatively small compared with the generated one. If the constants of 0.50 and 0.07 for  $f_b^{FBX}$  and  $(\Delta V/V)_e^{FBX}$  are used, no diffusion gas release is predicted to take place during the entire lifetime of operation because the centerline temperature is lower than the threshold one and thus no thermal feedback effect occurs.

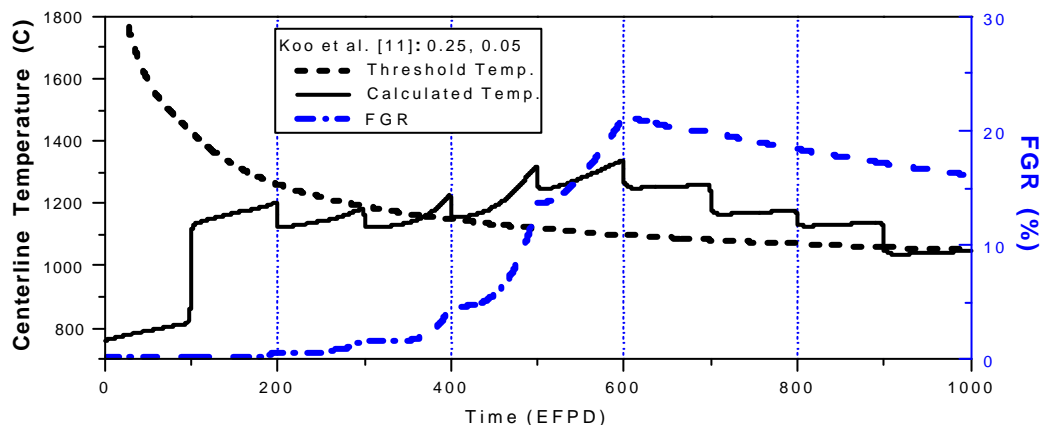


Fig4. Analysis of Koo et al's FGR model [11] using case 14 in Table 3 for MOX-1.

## 4. Uncertainty

### 4.1. Microstructure

Detailed information on the microstructure of the MOX fuel to be used in the test will be available after a report on the analytical work for MOX pellet is prepared. Until then, it is assumed that the microstructure of the MOX fuel is homogeneous without producing any significant difference in overall in-pile thermal behavior compared with  $\text{UO}_2$  fuel due to the addition of Pu.

### 4.2. Thermal conductivity

According to a recent analysis [14], the thermal conductivity of MOX fuel is best fitted if a constant 0.92 is multiplied by a thermal conductivity for  $\text{UO}_2$  fuel [15]. However, the fitting constants varied between 0.8 and 1.0 [14] depending on fuels. The thermal conductivity of MOX pellets to be used in the test is planned to be measured for all pellet batches for the purpose of comparison between thermal conductivity for fresh MOX fuel and the one derived from measured data during and/or after irradiation. Until these measurement results are available, it is assumed that the MOX fuel would take one of the three thermal conductivities corresponding to 1.00, 0.95, or 0.90 times the  $\text{UO}_2$  thermal conductivity.

### 4.3. Linear power

There are several sources of uncertainties that could contribute to the uncertainty of the linear power of the test rods and thus it is assumed for simplicity that the linear power has a 5% of uncertainty on the basis of the preliminary one; that is, the linear power would be one of the 1.05, 1.00, or 0.95 times the preliminary linear power.

### 4.4. Manufacturing parameters

Table 2 in Sec.3.1 shows some of the manufacturing tolerances that are applicable to the three MOX rods. Although fuel manufacturing has not yet finished, final manufacturing data would exist between the lower and upper extremes of tolerances. It is assumed that manufacturing parameters would take one of the nominal, maximum (nominal + tolerance), or minimum (nominal - tolerance) value. In Table 2, "*Max*" means that manufacturing tolerances are combined in such a way that the highest fuel centerline temperature is obtained and "*min*" indicates that manufacturing tolerances are combined so that the lowest fuel centerline temperature is achieved.

### 4.5. Model constants

Best-estimate model constants are derived so that they can best fit the measured data from which the model constants are derived. On the contrary, upper and lower bound model constants are determined in such a way that all the calculated values lie above or below the measured ones, respectively. Model constants would normally have values between upper and lower bound ones. It would be most probable that they take the constants close to the best-estimate ones. Three cases will be considered in this paper: first, a case that model constants are best-estimate, second, a case that the model constants are combined so that the highest fuel centerline temperature can be obtained (designated as "*Upper*" in the Table 3 of Sec.5.1), and finally a case that the model constants are combined so that the lowest fuel centerline temperature can be achieved, which is designated as "*Lower*" in the Table 3.

## 5. Calculation and discussion

### 5.1. Calculational cases

The total of seventeen calculational cases in Table 3 are chosen to investigate the in-pile behavior of the three MOX rods in the Halden reactor. They can be classified into 5 groups according to which parameters are mainly varied. Group 1 investigates the effect of uncertainty in MOX fuel's thermal conductivity on overall thermal performance for nominal linear power, nominal manufacturing parameters and best-estimate model constants. On the other hand, groups 2 and 3 examine the effect of uncertainty in thermal conductivity for the cases that linear power is 105% and 95% of its nominal value, respectively. Group 4 is selected mainly to study the influence of uncertainty in manufacturing parameters while changing the thermal conductivity and linear power simultaneously so that this group can cover the cases that might happen during irradiation. Finally, group 5 deals with the cases how the selection of the model constants would affect in-pile performance of MOX fuel.

Table 3. Seventeen calculation cases considering uncertainties.

Case No.		Thermal conductivity	Linear power	Manufacturing parameters	Model constants
Group 1	1	1.00	1.00	Nominal	Best-estimate
	2	0.95	1.00	Nominal	Best-estimate
	3	0.90	1.00	Nominal	Best-estimate
Group 2	4	1.00	1.05	Nominal	Best-estimate
	5	0.95	1.05	Nominal	Best-estimate
	6	0.90	1.05	Nominal	Best-estimate
Group 3	7	1.00	0.95	Nominal	Best-estimate
	8	0.95	0.95	Nominal	Best-estimate
	9	0.90	0.95	Nominal	Best-estimate
Group 4	10	0.95	1.00	<i>Max</i>	Best-estimate
	11	0.95	1.00	<i>min</i>	Best-estimate
	12	0.90	1.05	Max	Best-estimate
	13	1.00	0.95	min	Best-estimate
Group 5	14	0.95	1.00	Nominal	<i>Upper</i>
	15	0.95	1.00	Nominal	<i>Lower</i>
	16	0.90	1.05	Nominal	Upper
	17	1.00	0.95	Nominal	Lower

## 5.2. Calculational results

### 5.2.1. Results for MOX-1

Fig.5 shows the calculation results for all 17 cases in descending order of fuel centerline temperature and Fig.6 displays centerline temperatures for six cases that have a high probability of taking place during irradiation. It is interesting to note that, as can be seen in Fig.7, the four cases of high fuel temperature are related to high fission gas release resulting in reduced gap conductance. This suggests that, depending on whether the fuel centerline temperature exceeds the threshold temperature or not, the thermal performance of fuel can make a very big difference through the gap conductance. From the calculations, very high internal pressure implies that they can reach up to the value which the equipped pressure transducer may not measure because the bellows in the pressure transducer can not be compressed any further. Another seventeen calculations were also performed for the MOX-1 with the FGR model constants of 0.50 and 0.07 for  $f_b^{FGR}$  and  $(\Delta V/V)_g^{FGR}$ , and their results are similar to those for Fig.7. However, since more fission gas atoms can be retained in the grain boundaries due to increased  $f_b^{FGR}$  and  $(\Delta V/V)_g^{FGR}$ , lower fuel centerline temperatures are obtained.

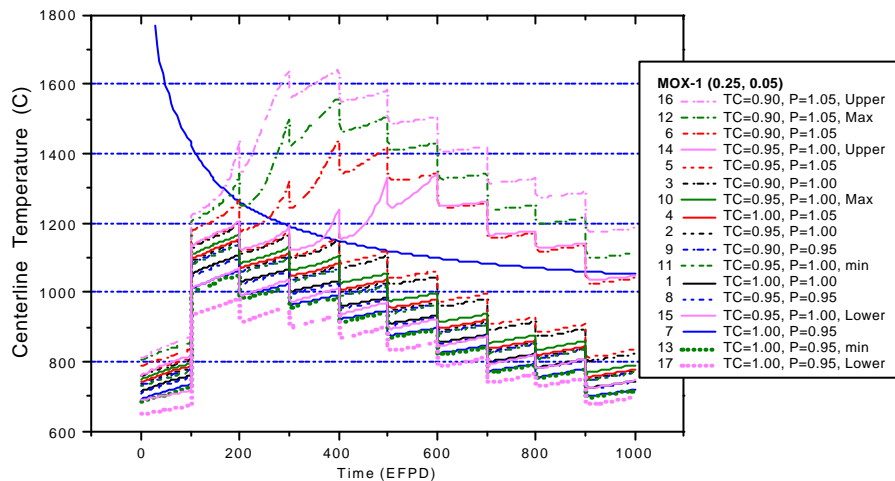


Fig.5. Fuel centerline temperatures for 17 calculational cases in MOX-1 for FGR model constants of 0.25 and 0.05.

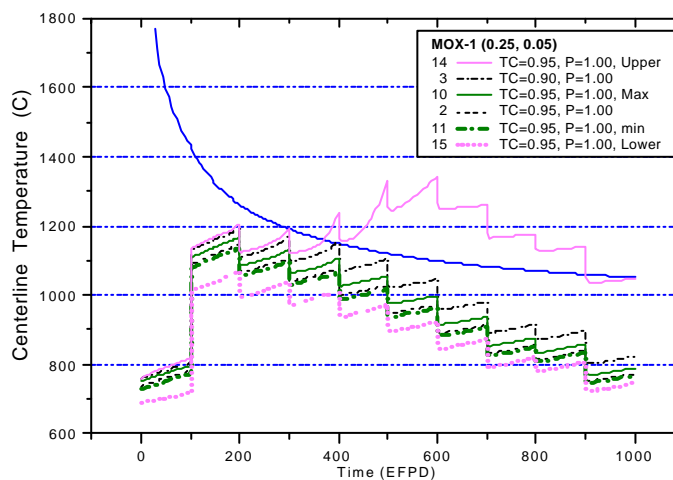


Fig.6. Centerline temperatures for six cases with high probability of occurrence in MOX-1 for FGR model constants of 0.25 and 0.05.



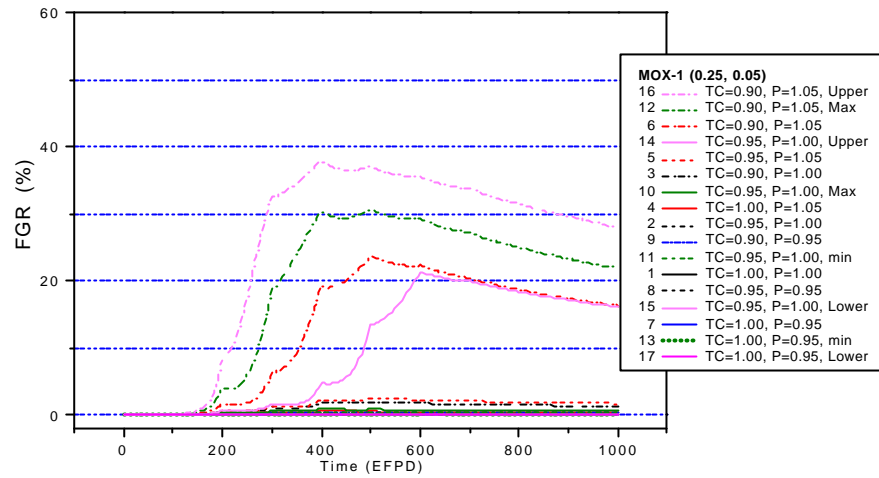


Fig.7. Fission gas releases (FGR) for 17 calculational cases in MOX-1 for FGR model constants of 0.25 and 0.05.

### 5.2.2. Results for MOX-3

The thermal performance of the MOX-3 and MOX-1 is different in three respects; first, the fuel temperature of the MOX-3 is higher than the MOX-1 for the same linear power. While the former, which uses a thermocouple to measure the fuel centerline temperature, does not have a central hole for the entire fuel column except for 4 pellets at the upper part, the latter has a hole along its full length for the installation of an expansion thermometer. Second, as seen in Fig.2, linear power of the MOX-3 is slightly higher than the MOX-1 during the lifetime in the Halden reactor. Finally, since the fabrication methods are different, microstructure of the two MOX rods, for example thermal conductivity, would be also different. The effect of these three factors on thermal performance, which is enhanced by positive thermal feedback, would be to yield a higher fuel temperature in the MOX-3 releasing more gas atoms.

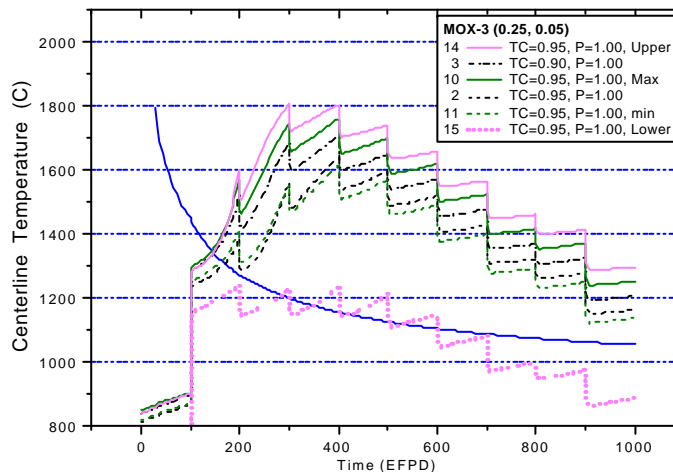


Fig.8. Centerline temperatures for six cases with high probability of occurrence in MOX-3 for FGR model constants of 0.25 and 0.05.

Fuel centerline temperatures calculated with the FGR model constants of 0.25 and 0.05 for  $f_g^{THER}$  and  $(\Delta V/V)_g^{THER}$ , as shown in Fig.8, are higher than the threshold temperatures for 6

cases that are likely to occur with high probability during operation. Fig.9 indicates that even in the case of 15 where "Lower" model constants are combined with 95% thermal conductivity and nominal power, there exists some diffusional gas release. This implies that it is very probable that the centerline temperature can go beyond the threshold temperature if the thermal conductivity of the MOX-3 corresponds to 95% of UO<sub>2</sub> fuel.

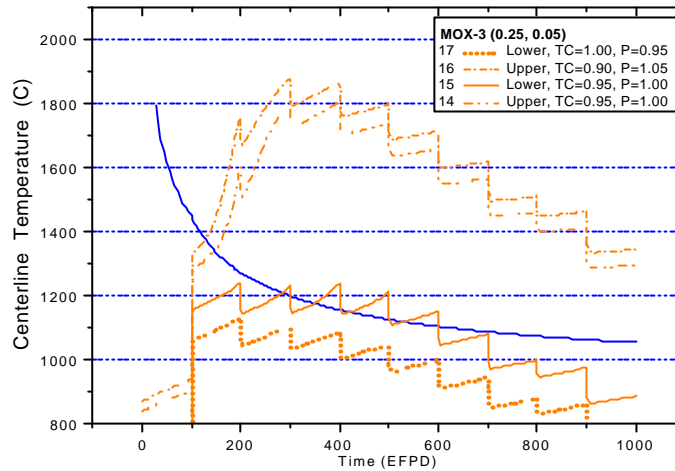


Fig.9. Effect of model constants on centerline temperature in MOX-3 for FGR model constants of 0.25 and 0.05.

Therefore, during the first cycle irradiation when there is no gas release due to low linear power (low fuel temperature) and hence gap conductance is not reduced significantly through the contamination of initially filled He gas with released gas, the centerline temperature should be analyzed closely to derive the thermal conductivity *in situ* of the MOX-3 so that it can be used to predict fuel performance during the subsequent cycles where linear power reaches up to 340 W/cm, which is high enough to yield diffusional gas release.

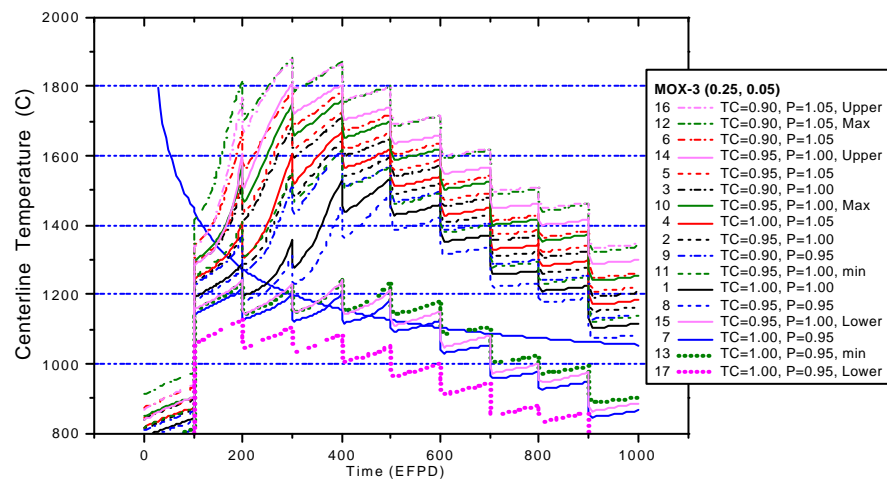


Fig.10. Fuel centerline temperatures for 17 calculational cases in MOX-3 for FGR model constants of 0.25 and 0.05.

In the case that FGR model constants of 0.50 and 0.07 are used for  $f_b^{TJEX}$  and  $(\Delta V/V)_e^{TJEX}$ , it is expected that, due to a larger amount of gas inventory that can be retained in the grain boundaries, both gas release and fuel centerline temperature would be lower than those results

shown in Fig.8. However, the difference between the two is not as large as expected. This is because the capacity of grain boundaries to retain gas atoms is not large enough to accommodate the large amount of gas atoms reaching the grain boundaries through diffusion. It is to be noted that, from Fig.5 and Fig.10, the orders by which centerline temperatures are displayed are slightly different. This difference arises because the effect of positive thermal feedback on fuel temperature is a function of many parameters such as the amount of gas release, densification, swelling and so on.

## 6. Summary

Considering four kinds of uncertainties – thermal conductivity, linear power, manufacturing parameters, and model constants – parametric studies have been made to investigate the effect of each uncertainty on in-reactor behavior. It is found that the uncertainty of model constants for FGR has the greatest impact on thermal performance of all because the amount of gas released to the gap strongly affects the gap conductance through the contamination of initially filled He gas. In the present analysis, two sets of model constants for FGR model have been used.

The parametric analysis shows that, in the case of the MOX-1, calculational results vary widely depending on the choice of model constants for FGR. Therefore, the model constants for FGR for the test need to be established through the measured fuel centerline temperature, rod internal pressure, stack length if any, and finally thermal conductivity derived from measured data during irradiation. On the other hand, the thermal performance of the MOX-3 depending on the choice of FGR model constants is not as large as that for the MOX-1. This happens because the capacity of grain boundaries to retain gas atoms is not large enough to accommodate the large amount of gas atoms reaching the grain boundaries through diffusion.

It is planned that when the data on the microstructure and thermal conductivity for each type of MOX fuel are available, new analysis will be made based on this information. In addition, FGR model constants will be derived from the measured centerline temperature, rod internal pressure and other related data.

## Acknowledgements

The authors would like to express their appreciation to the Ministry of Science and Technology (MOST) of the Republic of Korea for the support of this work through the mid- and long-term nuclear R&D Project.

## References

- [1] Yang-Hyun Koo, Byung-Ho Lee and Dong-Seong Sohn, "COSMOS: A computer code to analyze LWR UO<sub>2</sub> and MOX fuel rod", Journal of the Korean Nuclear Society, Vol.30 (1998) 541-554.
- [2] Uwe Kasemeyer, "Specification of the IMF/MOX experiment in the HBWR", CP-Note99-8, April 1999.
- [3] Hyung-Kook Joo, "Preliminary nuclear design for IMF-MOX fuel irradiation test in the Halden Boiling Water Reactor", KAERI, Dec.1998.
- [4] Dong-Seong Sohn et al., "Draft drawing and dimension for MOX test rods in the Halden Reactor", KAERI, January 1999.
- [5] G. Gates, "Supply of SBR MOX fuel for the IMF-MOX fuel irradiation in the Halden Reactor",

Halden internal memo, February 26, 1999.

- [6] Hyung-Kook Joo, "Calculational file for power histories of three MOX and three IMF fuel rods to be irradiated in the Halden Boiling Water Reactor", KAERI, June 1999.
- [7] Dong-Seong Sohn et al., "Fuel design report for 14x14 assembly", KAERI/SIEMENS, Nov. 1987.
- [8] Yang-Hyun Koo et al., "Radial power density distribution of MOX fuel rods in the HBWR", KAERI/TR-1365/99, KAERI, July 1999.
- [9] K. Takano, "The MOX fuel behavior test IFA-5974/5: Temperature and pressure data to a burnup of 15 MWd/kgMOX", HWR-605, April 1999.
- [10] Private communication with Mr. W. Wisenack, Halden Project Manager.
- [11] Yang-Hyun Koo, Byung-Ho Lee and Dong-Seong Sohn, "Development of a mechanistic fission gas release model for LWR UO<sub>2</sub> fuel under steady-state conditions", Journal of the Korean Nuclear Society, Vol.28 (1996) 229-246.
- [12] W. Hering and J. Stackmann, "CARO-D: Fission gas release model", Siemens/KWU technical report, B111/e145/80, Aug. 1980.
- [13] P. Strijov, Yang-Hyun Koo and Dong-Seong Sohn, "Development of a fission gas release model for MOX fuel and its verification with the FIGARO program", KAERI/TR-1106/98, KAERI, July 1999.
- [14] G. Gates, K Takano and R.J. White, "Thermal performance of MOX fuel", HWR-589, March 1999.
- [15] W. Wiesenack, "Assessment of UO<sub>2</sub> conductivity degradation based on in-pile temperature data", ANS Topical Meeting on LWR Fuel Performance, Portland, Oregon, March 2-6, 1997.
- [16] C. Vitanza, E. Kolstad and U. Graziani, "Fission gas release from UO<sub>2</sub> pellet fuel at high burnup", ANS Topical Meeting on LWR Fuel Performance, Portland, Oregon, April 29-May 3, 1979.